

**Double photodetachment from the  $\text{Cl}^-$  ion**

A. Aguilar\* and J. S. Thompson

*Department of Physics, MS 220, University of Nevada, Reno, Nevada 89557-0058, USA*

D. Calabrese

*Department of Physics, Sierra College, Rocklin, California 95677, USA*

A. M. Covington

*Lake Tahoe Community College, South Lake Tahoe, California 95150-4524, USA*

C. Cisneros

*Centro de Ciencias Físicas, Universidad Nacional Autónoma de México, Cuernavaca 62131, Mexico*

V. T. Davis

*Photonics Research Center, United States Military Academy, West Point, New York 10996, USA*

M. S. Gulley

*LANSCE Division, Los Alamos National Laboratory, Los Alamos, New Mexico 87545, USA*

M. Halka

*Department of Physics, Embry-Riddle Aeronautical University, Prescott, Arizona 86301, USA*

D. Hanstorp and J. Sandström

*Department of Physics, Chalmers University of Technology and Göteborg University, SE-41296, Göteborg, Sweden*B. M. McLaughlin<sup>†</sup>*Department of Applied Mathematics and Theoretical Physics, The Queens University, Belfast BT7 1NN, United Kingdom*

D. J. Pegg

*Department of Physics, University of Tennessee, Knoxville, Tennessee 37996, USA*

(Received 25 September 2003; revised manuscript received 26 November 2003; published 25 February 2004)

The correlated process involving the photodetachment of two electrons from the  $\text{Cl}^-$  ion has been investigated over the photon energy range 20–45 eV. In the experiment, a beam of photons from the Advanced Light Source (ALS) was collinearly merged with a counterpropagating beam of  $\text{Cl}^-$  ions from a sputter ion source. The  $\text{Cl}^+$  ions produced in the interaction region were detected, and the normalized signal was used to monitor the relative cross section for the reaction. An absolute scale for the cross section was established by measuring the spatial overlap of the two beams and by determining the efficiency for collection and detection of the  $\text{Cl}^+$  ions. The overall magnitude and shape of the measured cross section for this process agrees well with an  $R$ -matrix calculation. The calculation identifies the dominant mechanism leading to the production of the  $\text{Cl}^+$  ion as being a direct nonresonant process involving the ejection of a pair of electrons from the valence shell. Less important is the indirect nonresonant process that involves the production and decay of core-excited and doubly excited states of the Cl atom in an intermediate step. Direct and indirect resonant mechanisms involving the excitation of a single  $3s$  core electron or more than one valence electron of the  $\text{Cl}^-$  ion were found to be insignificant in the energy range studied.

DOI: 10.1103/PhysRevA.69.022711

PACS number(s): 32.80.Gc

**I. INTRODUCTION**

Loosely bound systems such as negative ions are particularly well suited to explore the effects of electron correlation

on atomic structure and dynamics. The structure of a negative ion differs intrinsically from that of an atom or positive ion due to the nature of the force binding the outermost electron. In an atom or positive ion the valence electron moves asymptotically in the long-range Coulomb field of a positively charged core consisting of the nucleus shielded by the other electrons. This long-range binding potential is able to support an infinite spectrum of bound states. In contrast, the outermost electron in a negative ion experiences a short-range field arising from the polarization of an atomic core. Negative ions exhibit an enhanced sensitivity to correlation

---

\*Present address: National Institute of Standards and Technology, Gaithersburg, MD 20809, USA.

<sup>†</sup>Present address: ITAMP, Harvard Smithsonian Center for Astrophysics, Cambridge, MA 02138, USA.

effects due to the efficient suppression of the normally dominant long-range Coulomb force. The induced dipole potential associated with the short-range polarization force that binds the outermost electron is shallow and can only support a finite number of bound states. Typically, only a single state is bound in a negative ion. In general, photodetachment refers to a bound-free process in which one or more electrons can be ejected from a negative ion following the absorption of one or more photons. Multiphoton detachment processes require the use of an intense light source, such as a laser. Multielectron detachment processes induced by a single photon require the use of high-energy photons, such as those produced at a synchrotron radiation source.

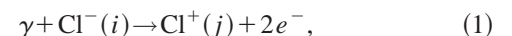
The subject of the present paper is the  $\text{Cl}^-$  ion, which has a closed  $3p$  subshell. As a consequence of the shell closing, the six valence electrons are relatively strongly bound. The electron affinity of the Cl atom was measured by Berzins *et al.* [1] to be 3.612724 eV. Due to this relatively large value, investigations of the laser photodetachment of  $\text{Cl}^-$  have primarily focused on multiphoton detachment processes involving the use of two or more photons to detach a single electron. The lowest-order process of single photon absorption-single electron detachment has received far less attention than is the case for most other ions. Trainham *et al.* [2] used a Penning trap and a laser to study one- and two-photon detachment from the  $\text{Cl}^-$  ion. Later, Blondel *et al.* [3] investigated four-photon detachment from  $\text{Cl}^-$  using a beam of ions and a laser. A similar multiphoton study that used six photons to detach an electron from  $\text{Cl}^-$  was reported by Davidson *et al.* [4]. Detachment processes need not, however, be restricted to the lowest-order process involving the ejection of a single electron. Multiple detachment involves the ejection of two or more electrons, typically following the absorption of a single photon. For example, the absolute cross sections for electron-impact detachment of one, two, and three electrons from  $\text{Cl}^-$  were measured recently by Fritioff *et al.* [5]. The subject of the present work, double photodetachment, is a highly correlated process in which two electrons are ejected from a negative ion following the absorption of a single photon. In this paper we describe a joint experimental and theoretical study of the absolute cross section for the production of  $\text{Cl}^+$  ions arising from the detachment of two electrons from the  $\text{Cl}^-$  ion.

There have been several previous investigations of cross sections for double photodetachment. Most of the studies have focused on threshold behavior or resonance structure. The first measurement of double photodetachment was made by Donahue *et al.* [6], who investigated the threshold behavior of the cross section for double detachment from the  $\text{H}^-$  ion. Similar measurements were made later on the metastable  $\text{He}^-$  ion by Bae *et al.* [7] and the stable  $\text{K}^-$  ion by Bae and Peterson [8]. All three experiments employed lasers to detach a pair of valence electrons. More recently, synchrotron radiation has been used to investigate more energetic processes involving inner-shell excitation and detachment from negative ions. Kjeldsen *et al.* [9] reported on the first measurement of a cross section for double photodetachment over an extended energy range. In this experiment the cross section for the production of  $\text{Li}^+$  ions following the absorption of a

single photon by the  $\text{Li}^-$  ion was measured over the energy range 45–62 eV. The cross-section measurement was absolute but the emphasis of the experiment was on the resonance structure in the cross section. The resonances in this case were associated with the autodetaching decay of  $K$ -shell core-excited states of  $\text{Li}^-$ . Similar studies of both the  $\text{Li}^-$  and  $\text{He}^-$  ions were made by Berrah *et al.* [10,11]. Gibson *et al.* [12] have recently investigated  $K$ -shell excitation in  $\text{C}^-$ . The double photodetachment cross section for the  $\text{Na}^-$  ion was measured by Covington *et al.* [13] over a photon energy range 30–51 eV. Again, the cross sections were absolute but the focus of the work was on determining the energies and widths of resonances in the cross section. In this case the observed resonances were associated with  $L$ -shell core-excited states of the  $\text{Na}^-$  ion. There have also been several theoretical treatments of double photodetachment. An early random phase approximation (RPA) calculation by Radojevic *et al.* [14] determined cross sections for single and multiple detachment from the negative ions of the halogens. More recently, both Zhou *et al.* [15,16] and Zatsarinny *et al.* [17] have used  $R$ -matrix methods to calculate photodetachment cross sections at energies corresponding to  $K$ -shell excitation. In the present paper, we report on an absolute measurement of the cross section for the production of  $\text{Cl}^+$  ions via double photodetachment of the closed shell negative ion,  $\text{Cl}^-$ . The data were accumulated over the photon energy range 20–45 eV. This range, which was dictated by the efficiency of the grating used to monochromatize the synchrotron radiation, encompasses the double detachment continuum from just above the threshold at the  $\text{Cl}^+(3p^4\ ^3P)$  limit up to the  $\text{Cl}^{2+}(3p^3\ ^4S^0)$  limit. The measured cross section is compared with predictions made using the  $R$ -matrix method.

## II. THEORY

Several distinct mechanisms have been identified that can lead to the production of a  $\text{Cl}^+$  ion when a  $\text{Cl}^-$  ion absorbs a photon in the energy range 20–45 eV. Both resonant and nonresonant processes are able to proceed either directly into the double detachment continuum or indirectly via the single detachment continuum. The mechanisms are shown schematically in Fig. 1. In the direct nonresonant process, labeled 1 in the figure, two valence electrons are detached from the  $\text{Cl}^-$  ion following the absorption of a single photon. The reaction can be written as



where  $(i)$  and  $(j)$  denote the internal energy states of the  $\text{Cl}^-$  and  $\text{Cl}^+$  ions, respectively. The initial state  $(i)$  is always the  $3s^23p^6\ ^1S$  ground state of  $\text{Cl}^-$  but the final state  $(j)$  may be the ground state or any excited state of  $\text{Cl}^+$ , depending on the energy of the absorbed photon. Over the range 20–40 eV, possible final-state configurations are  $3s^23p^4$ ,  $3s3p^5$ ,  $3s^23p^3nl$ , etc. (throughout this paper the Ne-like core will be omitted from configuration labels since it is inert in the range of photon energies used in this work). In the present experiment, the detection of the  $\text{Cl}^+$  ions was nonselective

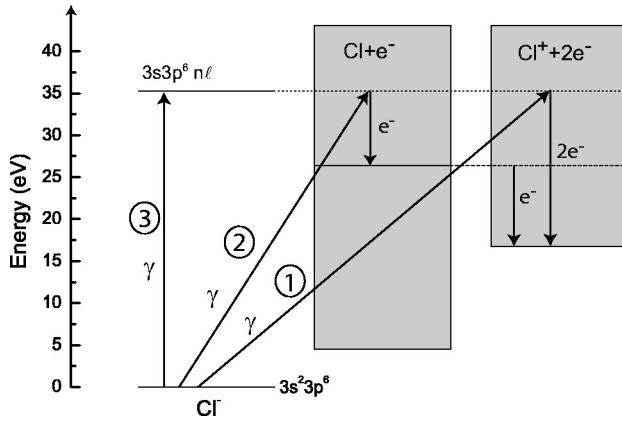
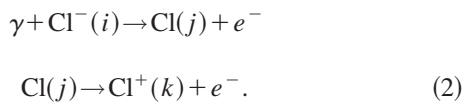


FIG. 1. An energy-level diagram covering the range of the experiment. It shows resonant and nonresonant transitions from the ground state of the  $\text{Cl}^-$  ion into the single and double detachment continua. The production of  $\text{Cl}^+$  ions via the direct and the indirect nonresonant processes are labeled 1 and 2, respectively. The direct and indirect resonant processes that result in the production of  $\text{Cl}^+$  ions are labeled 3.

with regard to the internal energy state. The data obtained in the experiment therefore represents the sum of all the partial cross sections associated with the different final states of  $\text{Cl}^+$ . The  $R$ -matrix calculation predicts that the direct nonresonant detachment of two valence electrons from  $\text{Cl}^-$  is the dominant process in the energy range studied, indicating a high degree of correlation between the six electrons in the closed  $3p$  subshell

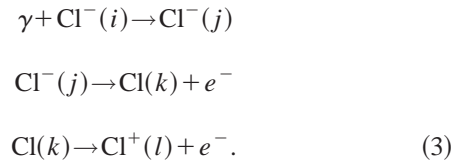
The indirect nonresonant process, labeled 2 in Fig. 1, involves the formation of an intermediate core-excited state or doubly excited state of the Cl atom. The nonresonant reaction is a two-step process that can be written as



Here  $(i)$ ,  $(j)$ , and  $(k)$  denote the internal energy states of the  $\text{Cl}^-$ , Cl, and  $\text{Cl}^+$  systems, respectively. The state  $(i)$  is again the  $3s^2 3p^6 \ ^1S$  ground state of  $\text{Cl}^-$ . A  $3s$  core vacancy in  $\text{Cl}^-$ , formed by detachment, is transferred to the Cl atom. The transient intermediate state of Cl is therefore a core-excited state, labeled  $(j)$  in Eq. (2). Core-excited states of Cl, for example, will have configurations of the type  $3s 3p^5 nl$ . It is also possible that the detachment of a single  $3p$  valence electron from  $\text{Cl}^-$  is accompanied by the excitation of two other  $3p$  electrons into higher orbitals. In this case the intermediate state  $(j)$  of the Cl atom would also be a doubly excited state with a configuration of the type  $3s^2 3p^3 nln'l'$ . A number of core-excited states and doubly excited states of Cl have been identified in the energy region from 20–40 eV in previous experiments involving the photoionization of the Cl atom [18,19] and collisions of  $\text{Cl}^-$  projectiles with gaseous targets [20,21]. In the second step shown in Eq. (2), the core-excited and doubly excited states of Cl decay by electron emission. The decay of a core-excited state is usually referred to as an Auger decay. Again, the final state  $(k)$  of the

$\text{Cl}^+$  ion will be either the ground state or an excited state, depending on the photon energy. In principle, a Cl atom in either core-excited or doubly excited states may also make a radiative transition to a bound state of the Cl atom, producing neutrals that are not detected in the experiment. However, the radiative branching is expected to be very small in the present case. The combined two-step, nonresonant process is represented in Fig. 1 by first a transition from the ground state of  $\text{Cl}^-$  into a single-electron detachment continuum, which results in the population of a core-excited or doubly excited state of Cl. These unstable states then rapidly decay into the two-electron detachment continua and the resulting  $\text{Cl}^+$  ions are detected. Some of the structure observed in the measured double photodetachment cross section is undoubtedly associated with this mechanism.

Resonant mechanisms may also contribute to the structure in the cross section. In these processes a core-excited state or a doubly excited state of the  $\text{Cl}^-$  ion is first produced by photoabsorption. This state is embedded in both the single and double detachment continua. In the direct resonant process the resonant state interacts with the double electron continuum and two electrons from the valence shell are detached. In the indirect resonant process the resonant state interacts with the single detachment continuum. The decay of the resonant state by autodetachment results in a single detached electron and a residual Cl atom that is left in a core excited or doubly excited state. The resonant two-step process can be written as



Here  $(i)$  and  $(j)$  denote the internal energy states of the  $\text{Cl}^-$  ion and  $(k)$  and  $(l)$  represent the internal energy states of Cl and  $\text{Cl}^+$ , respectively. At certain photon energies, the  $\text{Cl}^-$  ion will be excited from its  $3s^2 3p^6 \ ^1S$  ground state into a core-excited or multiply excited state of  $^1P$  symmetry with configurations of the type  $3s 3p^6 nl$ ,  $3s^2 3p^4 nln'l'$ , or  $3s^2 3p^3 nln'l'n''l''$ . Such states are embedded in one-electron detachment continua. Their decay will populate corresponding core-excited and doubly excited states of the Cl atom, as in the nonresonant process. These states, in turn, are embedded in two-electron detachment continua and their decay by electron emission will produce  $\text{Cl}^+$  ions in a variety of states. Double detachment in the energy range 20–40 eV involves the ejection of either two  $3p$  valence electrons or a single  $3s$  core electron and a single  $3p$  valence electron. The combined direct and indirect resonant processes are labeled 3 in Fig. 1.

The  $R$ -matrix method was used in this study to calculate the cross section over the range of energies used in the experiment. This theoretical method was initially developed to study electron-atom scattering [22]. However, in the half-collision concept the processes of photodetachment and electron-atom scattering are equivalent, and so the  $R$ -matrix method has also been used effectively on many occasions to

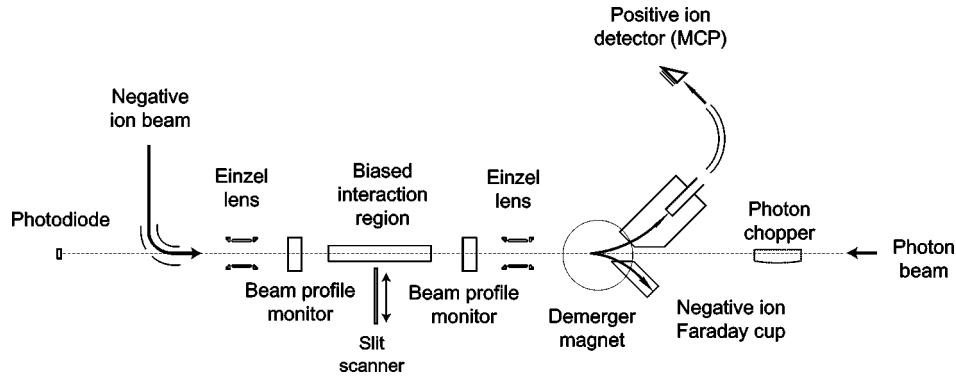


FIG. 2. A schematic of the apparatus showing the counterpropagating beams of negative ions from the ion source and photons from the synchrotron source. The collinearly merged beams interact in the biased interaction region. The spatial overlap of the two beams is measured by the beam profile monitors.

describe the process of photodetachment. In the present calculation of the cross section for the production of  $\text{Cl}^+$  ions from  $\text{Cl}^-$  ions in the double photodetachment process we employed an  $n=3$  physical orbital basis and used multiconfigurational expansions of the neutral Cl atom state in the scattering calculation. The  $1s$ ,  $2s$ ,  $2p$ ,  $3s$ , and  $3p$ , Hartree-Fock orbitals of Clementi and Roetti [23] were employed in the calculation. An additional  $3d$  orbital was included. The parameters associated with the  $3d$  orbital were determined by energy optimization on the appropriate spectroscopic state using the CIV3 structure code of Hibbert [24]. Details of this energy optimization process is given in the work of Ohja and Hibbert [25] and will not be elaborated on here. The aforementioned spectroscopic  $n=3$  basis that was used in the calculation will be referred to as basis *A*.

The electric-dipole selection rules limit the final states to  $^1P^0$  symmetry since the ground state of  $\text{Cl}^-$  has  $^1S$  symmetry. Hence, in the L-S coupling scheme, only doublet states of the neutral Cl complex can couple to the outgoing continuum electron ( $\epsilon_s, \epsilon_p, \epsilon_d, \dots$ ) to yield the  $^1P^0$  scattering states. Photodetachment cross sections were determined in the L-S coupling scheme using scattering codes developed for the International *R*-Matrix/Opacity Iron Project and the RmaX project [26–28]. The wave functions representing the scattering state were generated by allowing three-electron promotions out of specific base configurations. The neutral Cl target states (36 in total) that were included in our work, using basis *A*, were generated from the following electron configurations (the Ne-like core is inert in the energy range studied in the experiment and is therefore suppressed in the notation):  $3s^23p^5$ ,  $3s^23p^43d$ ,  $3s3p^6$ ,  $3s3p^43d^2$ ,  $3s^23p^33d^2$ , and  $3s3p^53d$ . The scattering calculations were carried out using 40 continuum orbitals, which were Lagrange orthogonalized to these physically bound orbitals. In the *R*-matrix photodetachment calculations a boundary radius of 35.8 Bohr radii was required to contain the electron density of the  $n=3$  basis. Triple electron promotions from these base configurations were used to represent wave functions of the scattered electron. In the outer region, the calculation of the scattering of an electron from the Cl atom were carried out with an energy mesh sufficiently fine (approximately, 1.36 meV) to resolve any narrow resonance structure

that might be present in the double photodetachment cross section. No narrow resonances were predicted in the 20–42 eV range used in the experiment but several strong and narrow resonances were predicted just below 20 eV.

In order to calculate the contribution from the direct double photodetachment cross section alone, we added together only those partial cross sections involving final states that lie above the  $\text{Cl}^+(3s^23p^4)$  ground-state threshold. The calculated electron affinity of 3.23 eV was in reasonable agreement with the accepted experimental value of 3.612 724 eV [1].

### III. EXPERIMENTAL PROCEDURE

In the experiment, we used the 10.0.1 undulator beamline at the ALS synchrotron radiation facility situated at the Lawrence Berkeley National Laboratory. The measurement was performed at the ion-photon-beam endstation, 10.0.1.2. A schematic of the apparatus is shown in Fig. 2. A more detailed description of the apparatus can be found in a recent paper by Covington *et al.* [29]. A beam of negative ions from a low-energy accelerator was collinearly overlapped with a beam of vacuum ultraviolet photons from the synchrotron source. The two beams were merged in a counterpropagating geometry. The  $\text{Cl}^-$  ions were produced in a sputter ion source, extracted at an energy of 5 keV, and focused by means of a series of cylindrical electrostatic lenses. The ion beam was then momentum selected using a  $60^\circ$  analyzing magnet. The cross-sectional area of the ion beam was defined by a pair of adjustable slits mounted in a plane perpendicular to the direction of propagation of the ion beam. The ion beam was then merged onto the axis of the counterpropagating photon beam using a set of  $90^\circ$  spherical sector bending plates. The primary ion beam then entered a 29.4 cm long cylindrical interaction region which was biased at +2 kV in order to energy label the  $\text{Cl}^+$  ions produced as a result of the photon-ion interaction. These ions had an energy of 9 keV after they left the interaction region. The energy labeling of the  $\text{Cl}^+$  ions produced by photodetachment enabled us to distinguish them from the  $\text{Cl}^+$  ions produced in double detachment collisions of  $\text{Cl}^-$  ions with the residual gas along the unbiased region of the beam line since they had an en-

ergy of 5 keV. The collisional background contribution was also reduced by maintaining a vacuum of  $5 \times 10^{-10}$  torr in the beam line.

In the center of the interaction region, the spatial overlap between the ion and photon beams was measured using a stepping-motor-driven slit scanner. Rotating-wire beam-profile monitors were used just upstream and downstream of the interaction region to ensure that the two beams were well collimated over the entire interaction region. The fine tuning of the overlap of the two beams was achieved by using two sets of mutually perpendicular electrostatic steering plates mounted immediately behind the plates used to merge the ion beam onto the axis of the photon beam. This procedure allowed us to measure the beam overlap quantitatively and use it to establish an absolute scale for the cross-section data. The efficiency for the detection of the photoions was measured to be 0.62. Absolute measurements were made at seven different energies across the cross-section curve. A small correction was made to the photon energy scale to account for the Doppler shift associated with the moving ions.

After the interaction region, a  $45^\circ$  analyzing magnet was used to separate the energy-labeled positive ions produced by photodetachment in the interaction region from the primary negative ion beam and the positive ions produced in collisional detachment. The photoions had an energy of 9 keV, whereas most of the positive ions produced in collisions with the residual gas had an energy of 5 keV, as determined by the extraction voltage at the ion source. The photon beam was modulated at a frequency of 6 Hz using a computer-controlled shutter in order to discriminate against the small collisionally induced background of 9 keV positive ions created in the interaction region. The 9 keV photoions were further deflected, in the vertical dispersion plane, by use of a set of  $90^\circ$  spherical-sector bending plates. This was done to minimize any background arising from the collection of the primary negative ion beam. The dispersed  $\text{Cl}^+$  photoions then entered a negatively biased box surrounding the detector. Inside the box, the ions struck a metal plate and produced secondary electrons. These secondary electrons were accelerated toward a microchannel plate detector operating with a positively biased anode. The pulses generated by the electrons were amplified and passed through a single-channel analyzer to discriminate against electronic noise. The output of the discriminator was converted to TTL pulses and counted with an I/O board in a PC-based data acquisition and control system. Typically, the  $\text{Cl}^-$  ion-beam current in the interaction region was several hundred nanoamperes. The magnitude of this current was monitored and used to normalize the yield of photoions. Similarly, the photon intensity was monitored for normalization purposes using a calibrated Si  $p$ - $n$  junction photodiode. The analog outputs of the monitors of the ion-beam and photon beam intensities were digitized and counted. The normalized photoion signal was proportional to the double detachment cross section.

#### IV. RESULTS

The measured cross section for the double photodetachment of  $\text{Cl}^-$  over the energy range 20–45 eV is shown in

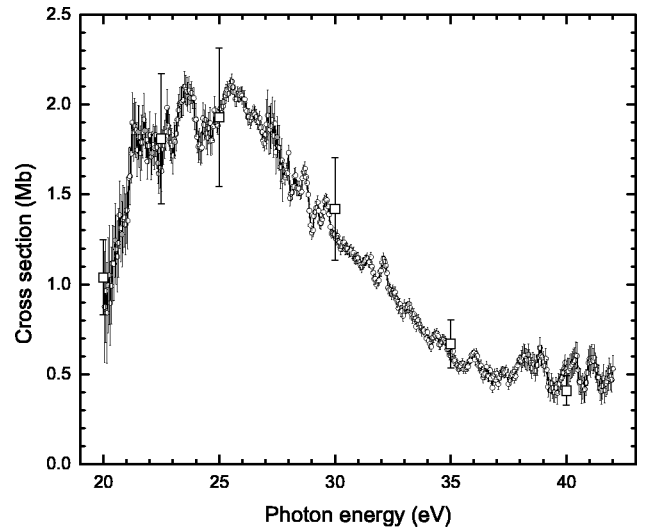


FIG. 3. The measured cross section for the production of  $\text{Cl}^+$  ions from  $\text{Cl}^-$  ions in the double photodetachment process. The cross-section scale was established by making absolute measurements (denoted by the open squares) at the six energies shown. The photon energy scale is measured relative to the ground state of  $\text{Cl}^-$ .

Fig. 3. The relative cross-section data were taken over the range 20–42 eV. The cross-section scale was established by making a series of seven absolute measurements over the range 20–45 eV. These data points are indicated by the open squares. The error bars on the absolute data points represent the systematic uncertainties in the measurements. These are estimated to be  $\pm 20\%$ . The threshold energy for the double photodetachment process in the case of  $\text{Cl}^-$  is 16.60 eV. Unfortunately, it was not possible to accumulate high-quality data below 20 eV in the present experiment due to the rapid drop-off in efficiency of the grating used to monochromatize the synchrotron radiation. Since the  $R$ -matrix calculation predicts strong resonances in the region just below 20 eV, we made a search for them in the experiment. Due to the low efficiency of the grating, the statistical quality of the data from 16–20 eV was poor. There was, however, a clear indication of the presence of several strong and narrow resonances. These resonances are associated with configurations of the type  $3s^2 3p^4 nln'l'$ . In Fig. 4 a comparison is made between the seven data points representing the measured absolute cross section and cross sections predicted by the  $R$ -matrix calculations. The photodetachment calculations involved 36 close-coupled states of the Cl atom using the  $n = 3$  basis set A. The upper theory curve contains contributions from both the direct and indirect processes that lead to  $\text{Cl}^+$  production following the absorption of a photon by a  $\text{Cl}^-$  ion. The lower curve represents only the direct process for  $\text{Cl}^+$ . It is clear from the figure that the direct process dominates the double photodetachment of  $\text{Cl}^-$  in this energy region.

The overall shape of the measured cross section agrees well with the present  $R$ -matrix calculation. The shape of the measured cross section also agrees with that of the previous RPA calculation of Radojevic *et al.* [14]. Again, the center of the relatively broad peak of the measured cross section is

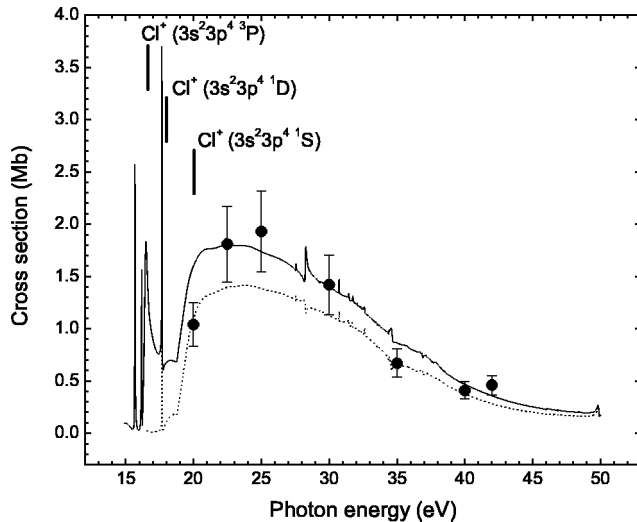


FIG. 4. Cross sections for the production of  $\text{Cl}^+$  ions from  $\text{Cl}^-$  ions via the process of double photodetachment. The lower dotted line represents the  $R$ -matrix calculation for the direct resonant and nonresonant processes. The addition of contributions from the indirect resonant and nonresonant processes results in the upper solid line. The seven data points represented by the circles are absolute measurements of the cross section. The photon energy scale is measured relative to the ground state of  $\text{Cl}^-$ . The energies of the ground and excited states of  $\text{Cl}^+$  are indicated by the small vertical lines.

slightly higher than that predicted by the RPA calculation. The magnitude of the measured cross section at its peak is about 2 Mb. The  $R$ -matrix calculation predicts a maximum cross section of about 1.8 Mb. Clearly, there is good agreement between the experiment and theory. The RPA calculation predicts a somewhat lower maximum cross section of about 1.2 Mb, which is outside of the experimental uncertainty.

The measured relative cross section shown in Fig. 3 has been smoothed, but still exhibits many weak and broad structures. It is suspected that the structure in the cross section in the range 20–42 eV arises from the direct and indirect resonant processes and indirect nonresonant process described in the theory section, but it is essentially impossible to distinguish between the resonant and nonresonant mechanisms at the present level of counting statistics. The nonresonant mechanism involves core-excited and doubly excited states of the Cl atom as intermediate states in the two-step decay process leading to the production of  $\text{Cl}^+$  ions. Many core-excited and doubly excited states of Cl are known to exist in the energy range of the present experiment. Much of the structure in the cross section is undoubtedly associated with these unstable states of Cl. Whenever the energy of the photon coincides with the energy of one of the core-excited states or doubly excited states of Cl, one expects there to be a step in the cross section associated with the threshold corresponding to the opening of a new continuum channel. The energies of core-excited states of Cl of the type  $3s3p^5nl$  have been determined in photoionization experiments by van der Meulen *et al.* [18], Cantu and Mazzoni [19], Thoft *et al.* [20], and Andersen *et al.* [21] in ejected electron spectra arising from collisions of  $\text{Cl}^-$  with rare-gas atoms. Such states

form Rydberg series that converge on the  $3s3p^5(^1,^3P)$  limits. The  $3s3p^5^3P$  state of  $\text{Cl}^+$ , for example, lies 28.17 eV above the ground state of the  $\text{Cl}^-$  ion. One therefore expects to find core-excited states of Cl with configurations of the type  $3s3p^5nl$  just below this energy. Similarly, a series of core-excited states should converge on the  $3s3p^5^1P$  parent state of  $\text{Cl}^+$ , which should lie a little higher in energy than the  $3s3p^5^3P$  state. There are indeed many structures in the measured cross section that might correspond to the opening of detachment continua associated with these states. There are fewer steplike features in the calculated cross section in this region. The  $R$ -matrix calculation is limited to a basis set that includes orbitals with principle quantum numbers not exceeding  $n=3$ , which explains why more structure is seen in the measured cross section than the calculated one. Thoft *et al.* [20] measured the energy of the  $3s3p^5(^1P)4s$  state to be 23.45 eV, with respect to the Cl ground state or 27.06 eV above the ground state of  $\text{Cl}^-$ . There is clearly structure in the measured cross section at this energy. Thoft *et al.* [20] also measured the energies of the  $3s3p^5(^1P)4p$  and  $3s3p^5(^1P)3d$  states to be 24.70 and 25.68 eV, respectively. These correspond to energies of 28.31 and 29.29 eV, respectively, relative to the  $\text{Cl}^-$  ground state. Again, there is structure in the measured cross section at these energies. The energies of members of the  $3s3p^5(^3P)np$  Rydberg series were measured in the photoionization experiment of van der Meulen [18]. They range from an energy of 25.681 eV for the  $n=4$  member to a series limit of 28.157 eV (all energies are relative to the ground state of  $\text{Cl}^-$ ). There is a lot of structure in the measured cross section over this energy range, some of which probably coincides with the core-excited states of the  $3s3p^5(^3P)np$  series. It is clear that there is a substantial overlap of the different Rydberg series and configuration interaction will preclude the use of pure single-electron configuration labels in some cases. The energies of doubly excited states of Cl of the type  $3s^23p^3nl'n'l'$  were also reported by van der Meulen *et al.* [18] and Thoft *et al.* [20]. In these states two electrons are coupled to the  $3s^23p^3(^4S, ^2D, ^2P)$  cores. One therefore expects many doubly excited states of Cl in the energy range 20–40 eV and some of the steplike structures in the measured cross section in this region are probably associated with these states. Eighteen unidentified resonances in the energy range 28.66–31.23 eV (with respect to the  $\text{Cl}^-$  ground state) were reported by van der Meulen *et al.* [18]. They are suspected to have configurations of the type  $3s^23p^3nl'n'l'$ . Thoft *et al.* [20] also measured the energies of doubly excited states with configurations of this type over the energy range 25.73–29.25 eV. These states involved  $4s$  and  $3d$  outer electrons.

Another source of structure in the double photodetachment cross section could be resonances associated with the formation and decay of core-excited or doubly excited states of  $\text{Cl}^-$ . At certain photon energies the  $\text{Cl}^-$  ion will be excited from its  $3s^23p^6^1S$  ground state into core-excited and multiply excited states of  $^1P^0$  symmetry with configurations of the type  $3s3p^6nl, 3s3p^5nl'n'l', 3s^23p^4nl'n'l'$ . The auto-detaching decay of such states give rise to corresponding states of the Cl atom. As mentioned earlier, these unstable intermediate states predominantly decay by electron emis-

sion to form  $\text{Cl}^+$  ions. A careful search for narrow resonances in the cross section was made under conditions of high-energy resolution and small step size. Only weak structures were observed and it is not clear in most cases whether they represent resonances or thresholds. The  $R$ -matrix calculation, which is limited to an  $n=3$  orbital basis set, does not predict strong resonances in the cross section in the range 20–45 eV. There are several possible explanations for the lack of prominent resonances in the  $\text{Cl}^-$  double photodetachment cross section. Core-excited states of negative ions usually interact most strongly with nearby continua, in which the autodetached electrons carry off only a small amount of energy. The corresponding partial cross sections will be the only ones that are strongly modulated by the resonance structure. If there are a lot of core-excited states of the Cl atom in the energy region studied, there will be many unresolved partial cross sections that are only weakly modulated. Under these conditions, the resonant structure in the few strongly modulated partial cross sections tends to get “washed out” in the summation. It is also possible that core-excited resonant states of  $\text{Cl}^-$  are strongly damped by the autodetaching decay process. In this energy region, resonant states of  $\text{Cl}^-$  will have a  $3s$  subshell vacancy. The lifetimes of core-excited states that involve  $3s$  vacancies could be rather short. If this is the case, the resonance may be broadened to such a degree that it becomes indistinguishable from the nonresonant cross-section background.

## V. SUMMARY

We have determined the cross section for double photodetachment leading to the production of  $\text{Cl}^+$  ions from  $\text{Cl}^-$  ions. The relative measurements were made over the range 20–42 eV. Seven absolute measurements were made over the range 20–45 eV.  $R$ -matrix calculations were performed over the energy range 16–45 eV. Four double detachment mechanisms leading to the production of  $\text{Cl}^+$  ions have been identified: two nonresonant processes and two resonant processes. The resonant processes do not appear to make a

significant contribution to the cross section at the energies studied in the experiment. The  $R$ -matrix calculation predicts that the dominant nonresonant mechanism is the direct and highly correlated process of detaching a pair of valence electrons from the closed  $3p$  subshell of the  $\text{Cl}^-$  ion. Less significant is the indirect nonresonant process that involves the production and decay of intermediate core-excited and doubly excited states of the Cl atom. The large number of such states in Cl appear, however, to be responsible for much of the steplike structure seen in the measured cross section. The magnitude and shape of the measured absolute cross section agrees well with the present  $R$ -matrix calculation.

Multiple electron detachment following the absorption of a single high-energy photon is a process that can yield important information on the structure and dynamics of negative ions. In general, this highly correlated process involves the ejection of two or more valence electrons and/or the ejection of one or more inner-shell electrons. In the near future, we intend to extend the present measurements involving the detachment of two electrons from  $\text{Cl}^-$  to the higher-order process in which three or more electrons are detached.

## ACKNOWLEDGMENTS

The work at ALS is supported by the U.S. Department of Energy under Contract No. DE-AC03-76SF00098. We would like to thank Ron Phaneuf for facilitating the ion-photo-beam (IPB) endstation for the experiment. The IPB is supported by the Division of Chemical Sciences, Biosciences, Geosciences of the U.S. Department of Energy under Contract No. DE-FG03-ER14787 with the University of Nevada, Reno (UNR). A.A. acknowledges support from UNR, DGAPA-UNAM, and from the ALS. C.C. acknowledges support from DGAPA-UNAM and CONACyT. D.H. and J.S. acknowledge support from the Swedish Research Council. V.D. acknowledges support from the US Army Research Office. B.M.McL. would like to thank the Institute for Theoretical Atomic and Molecular Physics for the hospitality and support under the visitors program. We would like to thank Gleb Gribakin for valuable discussions.

- 
- [1] U. Berzins, M. Gustafsson, D. Hanstorp, A. Klinkmüller, U. Ljungblad, and A.-M. Mårtensson-Pendrill, *Phys. Rev. A* **51**, 231 (1995).
  - [2] R. Trainham, G. Fletcher, and D. Larson, *J. Phys. B* **20**, L777 (1987).
  - [3] C. Blondel and R. Trainham, *J. Opt. Soc. Am. B* **6**, 1774 (1989).
  - [4] M.D. Davidson, D.W. Schumacher, P.H. Bucksbaum, H.G. Muller, and H.B. van Linden van den Heuvell, *Phys. Rev. Lett.* **69**, 3459 (1992).
  - [5] K. Fritioff, J. Sandström, D. Hanstorp, A. Ehlerding, M. Larsson, G.F. Collins, D.J. Pegg, H. Danared, A. Källberg, and A.L. Padellec, *Phys. Rev. A* **68**, 012712 (2003).
  - [6] J.B. Donahue, P.A.M. Gram, M.V. Hynes, R.W. Hamm, C.A. Frost, H.C. Bryant, K.B. Butterfield, D.A. Clark, and W.W. Smith, *Phys. Rev. Lett.* **48**, 1538 (1982).
  - [7] Y.K. Bae, M.J. Coggiola, and J.R. Peterson, *Phys. Rev. A* **28**, 3378 (1983).
  - [8] Y.K. Bae and J.R. Peterson, *Phys. Rev. A* **37**, 3254 (1988).
  - [9] H. Kjeldsen, P. Andersen, F. Folkmann, B. Christensen, and T. Andersen, *J. Phys. B* **34**, L353 (2001).
  - [10] N. Berrah *et al.*, *Phys. Rev. Lett.* **87**, 253002 (2001).
  - [11] N. Berrah, J.D. Bozek, G. Turri, G. Akerman, B. Rude, H.-L. Zhou, and S.T. Manson, *Phys. Rev. Lett.* **88**, 093001 (2002).
  - [12] N.D. Gibson, C.W. Walter, O. Zatsarinny, T.W. Gorczyca, G.D. Akerman, J.D. Bozek, M. Martins, B.M. McLaughlin, and N. Berrah, *Phys. Rev. A* **67**, 030703(R) (2003).
  - [13] A.M. Covington *et al.*, *J. Phys. B* **34**, L735 (2001).
  - [14] V. Radojevic, H.P. Kelly, and W.R. Johnson, *Phys. Rev. A* **35**, 2117 (1987).
  - [15] H.-L. Zhou, S.T. Manson, L.V. Ky, N. Feautrier, and A. Hibbert, *Phys. Rev. Lett.* **87**, 023001 (2001).

- [16] H.L. Zhou, S.T. Manson, L.V. Ky, A. Hibbert, and N. Feautrier, *Phys. Rev. A* **64**, 012714 (2001).
- [17] O. Zatsarinny, T.W. Gorczyca, and C.F. Fischer, *J. Phys. B* **35**, 4161 (2002).
- [18] P. van der Meulen, M.O. Krause, C.D. Calwell, S.B. Whitfield, and C.A. de Lange, *J. Phys. B* **24**, L573 (1991).
- [19] A.M. Cantu and M. Mazzoni, *Phys. Scr.* **43**, 472 (1988).
- [20] N.B. Thoft, T. Andersen, P. Dahl, and L. Jodal, *J. Phys. B* **28**, 1443 (1995).
- [21] T. Andersen, P. Dahl, J.E. Hansen, J. Poulsen, and N.B. Thoft, *J. Phys. B* **22**, L591 (1989).
- [22] P. G. Burke and K. A. Berrington, *Atomic and Molecular Processes: An R-matrix Approach* (IOP, Bristol, UK, 1993).
- [23] E. Clementi and C. Roetti, *At. Data Nucl. Data Tables* **14**, 177 (1974).
- [24] A. Hibbert, *Comput. Phys. Commun.* **9**, 141 (1975).
- [25] P. Ohja and A. Hibbert, *Phys. Scr.* **42**, 424 (1990).
- [26] M. Seaton, *J. Phys. B* **20**, 6363 (1987).
- [27] K.A. Berrington, W. Eissner, and P. Norrington, *Comput. Phys. Commun.* **92**, 290 (1995).
- [28] R-matrix codes: URL [http://amdpp.phys.strath.ac.uk/UK\\_RmaX](http://amdpp.phys.strath.ac.uk/UK_RmaX)
- [29] A. Covington *et al.*, *Phys. Rev. A* **66**, 062710 (2002).